Non-interferometric wavefront sensing technique for EUV Lithography system

A. Polo[1], F. Bociort[1], S.F. Pereira[1], H.P. Urbach[1]

[1] Technishe Universiteit Delft, Lorentzweg 1, 2628 CJ Delft, The Netherlands

The goal of creating lithographic-quality EUV imaging system has pushed research to develop the most accurate wavefront aberration measurement techniques ever created. During the past years many techniques have been developed based on interferometry but in spite of very high accuracy in aberration detection, these techniques presents a lot of disadvantages. In this work we are going to focus on a different technique that requires no interferometry but is based on the Hartmann Wavefront Sensor. We present a mathematical model of this system which demonstrates the feasibility and the possible advantages in term of dynamic range and accuracy of this technique compared to interferometric techniques.

Introduction

The semiconductor industry continues to derive profits and revenue from device scaling, hence every technique that promises to extend dimensional scaling receives great attention from the industry. Nowadays the process used in order to print a geometrical pattern on a semiconductor wafer is Optical Projection Lithography (OPL). The latest system uses light of 193 nm wavelength to transfer the pattern from a transmissive photo mask to a light-sensitive photo resist through an optical system with a reduction factor of $4\times$.
The smaller feature size that can be print is related to the resolution on the system given by

$$RES = k_1 \frac{\lambda}{NA} \tag{1}$$

where k_1 is an experimental parameter, λ the wavelength and NA the numerical aperture of the system. From Eq.1 is simple to notice that in order to improve the resolution a decrease of the wavelength of the light source, a decrease of the factor k_1 or an increase in NA is necessary. Extreme Ultraviolet Lithography (EUVL) is considered as the natural extension of OPL since it uses photons of 13.5 nm wavelength to carry out the imaging and it promise extendibility by addressing not only the 32 nm half-pitch nodes but several nodes beyond that[1]. However, in spite of similarities, there are many differences between the two optical systems for the old and the new wavelength because the material property for EUV are very different from those for 193 nm. For example, since EUV radiation is strongly absorbed in all materials and gases it is necessary to use Multilayer (ML) reflective mirrors in the projection optics instead of refractive lenses used in OPL (Fig.1). Furthermore, because of the short wavelength used to carry out the imaging, the surfaces of these mirrors should exhibit unprecedented levels of perfection. In order to achieve diffraction-limited imaging, it has been proved that the root-mean square (rms) wavefront error on each mirror must be accurate to 0.25 nm.[2] Moreover, due to the partial reflectivity of a ML mirror (maximum about 70%), deformations caused by radiation

absorption can occur on the mirror surface. This can cause aberrations in the EUV beam resulting in a loss of resolution and consequently a poor image quality projected on the wafer. In order to minimize all the systematic errors in a EUVL system it could be necessary, like in the astronomic telescope, to introduce an adaptive optics system to correct the aberrations in the optical system and achieve a perfect diffraction limited imaging. Therefore, a lot of research is currently done to develop a metrology technique that can measure the wavefront at such short wavelength with a very high accuracy.

Discussion

During the past years many techniques has been developed based on interferometry such as Point Shift Point Diffraction Interferometer[3] (PS/PDI) or Lateral Shearing Interferometer [4] (LSI) but in spite of very high accuracy in aberration detection (in the order of $\lambda/350$ for PS/PDI and $\lambda/135$ for LSI), these techniques present a lot of disadvantages such as very hard to setup, extreme demands on the temporally and spatially coherence of the beam under test, complex wavefront analysis and, not less important, a very limited dynamic range of the magnitude of aberrations that can be measured with them. In contrast, Hartmann wavefront (HWF) sensors have important advantages over interferometry in the EUV range[5]. With this technique, we can measure both phase and intensity at the same time. A HWF sensor can work with relaxed coherent requirements regarding the source. We can measure a widespread magnitude of aberration. Furthermore, this system is more compact, inexpensive and easy to build. In the HWF sensor (Fig.2), the beam under test passes through a grid that consists of a holes array and the shadow of the mask is projected onto a detector.

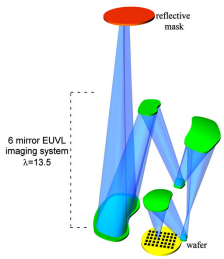

Figure 1: EUV lithography system

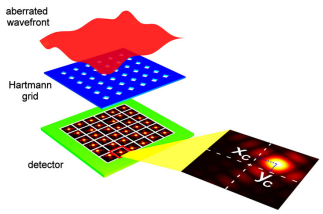

Figure 2: HWFS scheme

Aberration in the wavefront (slope) cause deviation in the projected beam resulting in a measurable shift of the individual spot centroid referred to the local slope of the wavefront, from which the wavefront can be reconstructed. The different holes in the grid are identified by two indices i and j, i associated with the x dimension and j with the y dimension. For each hole, the wavefront local slopes denoted by S^x_{ij} and S^y_{ij} are given by the following equations:

$$\begin{cases} S^x_{ij} = \frac{\partial W}{\partial x} = \frac{x_{c,ij} - x_{r,ij}}{L} \\ S^y_{ij} = \frac{\partial W}{\partial y} = \frac{y_{c,ij} - y_{r,ij}}{L} \end{cases} \tag{2}$$

where:

- x_c, x_r and y_c, y_r represent respectively the position of the measured and reference spot in the x and y position;
- L represents the distance between the sampling and detection planes.

The hole size is chosen in order to avoid overlap in the projected pattern in order to be clearly resolved. Depending on the geometrical property of the beam to be analyzed and the desired performance of the sensor, the hole sizes of the array of the Hartmann grid can vary from 30 μm to 120 μm with spacings from 60 μm to 300 μm.
In our simulation, the geometry of the Hartmann grid consist of an array with 44 $\times$ 44 holes over an 11×11 mm^2 area. The holes are squares with 80 μm size, spaced by 225 μm. Also each hole is rotated by 25 degree in order to minimize the overlap of the diffraction order from the adjacent hole in the measurement plane. The distance L between the grid and the image plane is set to 400 mm. With these parameters the field distribution on the image plane is to a very good accuracy approximated by the Fraunhofer pattern.
The aberration in the system is introduced as a phase distortion factor (in terms of a Zernike polynomial) that multiplies the Hartmann grid function according to the following equation:

$$U(x,y,0) = U_0 \exp[ikW(x,y)]G(x,y) \tag{3}$$

Where $U(x,y,0)$ is the complex field distribution across the $z=0$ plane, $W(x,y)$ define the aberration, $k = 2\pi/\lambda$, and $G(x,y)$ define the geometry Hartmann grid (i.e. G is 1 inside the holes and 0 between the holes). The algorithm consists of two main step:

- Detection of the spot displacement in the detector plane;
- Reconstruction of the wavefront from the calculated local slope of the wavefront.

In order to detect the spot displacement in the detector plane caused by the aberration, a center of mass algorithm is applied on each spot. Then the resulting x and y coordinate on each spot are compared with the case in which there are no aberrations. From these values, the local slopes are calculated using Eq.2.
Fig.3 shows an example of slope computation referred to astigmatism.

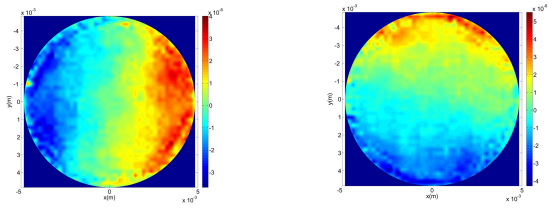

(a) (b)

Figure 3: 3(a) astigmatism wavefront slope in the x direction; 3(b) astigmatism wavefront slope in the y direction

Result

In this section results of the reconstruction of the wavefront from measured slopes from simulated data are shown. In particular we consider four types of aberrations: defocus, astigmatism, coma and a mixture of them.
Fig. 4 shows, for each type of aberration mentioned above, the reconstructed wavefront and its mismatch with the original one.

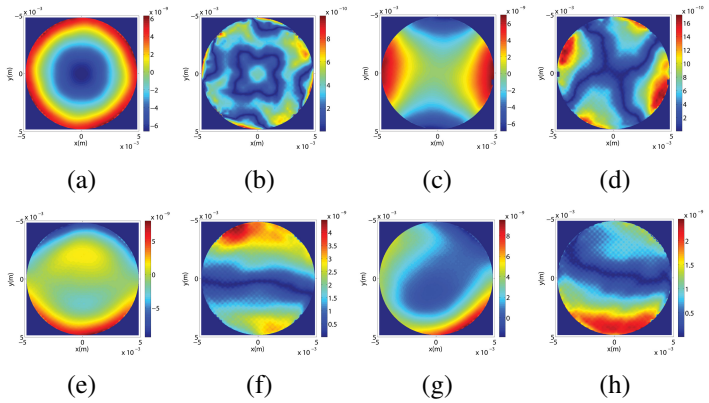

Figure 4: 4(a) reconstructed defocus; 4(b) defocus phase mismatch, rms=0.61 nm; 4(c) reconstructed astigmatism; 4(d) astigmatism phase mismatch, rms=0.79 nm; 4(e) reconstructed coma; 4(f) coma phase mismatch, rms=2.03 nm; 4(g) reconstructed mixture; 4(h) mixture phase mismatch, rms=1.1 nm

As we can see the main shape of the aberration is reconstructed but the reconstruction accuracy decrease as the complexity of the wavefront increase. In fact (see note in the figure caption) we can achieve the smaller rms wavefront of 0.61 nm in case of defocus but it increase to 2.2 nm in case of coma.

Conclusion

The purpose of the research is to investigate the advantages and possible constrains in the characterization of the wavefront using an Hartmann Wavefront Sensor working at 13.5 nm to be coupled in a EUV Lithography system. Further developments for improving the accuracy of the reconstruction algorithm and for an experimental validation of the mathematical model are currently under investigation.

References

[1] J.E. Bjorkholm *EUV lithography - The successor to Optical Lithography*. Intel Technology Journal Q3, 1998.

[2] Bakshi, V. *EUV Lithoraphy*. s.l. : Spie Press, 2009.

[3] P.P.Naulleau, K.A.Goldberg, S.H.Lee. *EUV Phase-shifting PDI: a wavefront metrology tool with subangstrom reference-wave accuracy*. Applied Optics, Vol. 38. n. 35, 1999

[4] J.E. Bjorkholm, A.A. MacDowell, O.R. Wood. *Phase-measuring Interferometry using extreme ultraviolet radiation*. American Vacuum Societ, 1995.

[5] P. Mercere, P. Zeitoun, M. Idir. *Hartmann Wavefront measurement at 13.4 nm with* $\lambda_{EUV}/120$ *accuracy*. Optics Letter, Vol. 28 n 17, 2003.